International Journal of Biological Macromolecules 61 (2013) 204–211

Contents lists available at SciVerse ScienceDirect

International Journal of Biological Macromolecules

journal homepage: www.elsevier.com/locate/ijbiomac

Molecular features determining different partitioning patterns of papain and bromelain in aqueous two-phase systems

Maria Victoria Rocha, Bibiana Beatriz Nerli*

Departamento Química-Física, Facultad de Ciencias Bioquímicas y Farmacéuticas, Universidad Nacional de Rosario, Suipacha 531 (S2002LRK), Rosario, Argentina

ARTICLE INFO

Article history:
Received 21 May 2013
Received in revised form 20 June 2013
Accepted 28 June 2013
Available online xxx

Keywords:
Aqueous two-phase systems
Papain
Bromelain
Protein–polymer interaction

ABSTRACT

The partitioning patterns of papain (PAP) and bromelain (BR), two well-known cysteine-proteases, in polyethyleneglycol/sodium citrate aqueous two-phase systems (ATPSs) were determined. Polyethyleneglycols of different molecular weight (600, 1000, 2000, 4600 and 8000) were assayed. Thermodynamic characterization of partitioning process, spectroscopy measurements and computational calculations of protein surface properties were also carried out in order to explain their differential partitioning behavior. PAP was observed to be displaced to the salt-enriched phase in all the assayed systems with partition coefficients (Kp_{PAP}) values between 0.2 and 0.9, while BR exhibited a high affinity for the polymer phase in systems formed by PEGs of low molecular weight (600 and 1000) with partition coefficients (Kp_{BR}) values close to 3. Kp_{BR} values resulted higher than Kp_{PAP} in all the cases. This difference could be assigned neither to the charge nor to the size of the partitioned biomolecules since PAP and BR possess similar molecular weight (23,000) and isoelectric point (9.60). The presence of highly exposed tryptophans and positively charged residues (Lys, Arg and His) in BR molecule would be responsible for a charge transfer interaction between PEG and the protein and, therefore, the uneven distribution of BR in these systems.

1. Introduction

Aqueous two-phase systems (ATPSs) formed by a polymer and a kosmotropic salt provide a powerful method for separating different bio-materials such as cells, organelles, nucleic acids and proteins [1,2]. Homogenates, culture media and crude supernatants containing both the target molecule and particulate materials - cells, cell debris- can be directly loaded into the ATPSs without a previous centrifugation or filtration step, integrating clarification and partial purification in one unit operation [3]. Extraction with ATPSs exhibits several advantages compared to other purification methods such as high capacity, short processing times and low cost, making the process easy to scale-up [4]. Despite these favorable features, ATPSs have not been extensively adopted in either industrial processes or commercial applications. The main reason for this could be attributed to the poor knowledge about the mechanisms involved in the partitioning equilibrium of macromolecules and consequently, the lack of a comprehensive theory able to predict the experimental trends. The uneven/even distribution of biomolecules in ATPSs is caused by two groups of factors [5]. One of them comprises those factors inherent to the system itself-type, molecular weight and concentration of phase forming polymers, type and concentration of salt and pH. The other includes those factors which depend on the characteristics of the partitioned molecule-molecular weight, pI, surface properties. Separation of a target molecule from other components in a complex mixture is achieved by manipulating the partitioning behavior by altering the average molecular weight of the polymers, the type of ions in the system, the ionic strength of the salt phase and the pH. Therefore, the application of the technique requires hit-or-miss experimentation to design an adequate phase system for optimal partitioning of a particular protein.

The most commonly used ATPSs for large-scale enzyme extraction are formed by polyethylenglycol (PEG) and phosphate or sulfate salts. Recently, those ATPSs containing a salt of a biodegradable anion have become particularly interesting due to their low environmental impact [6]. PEG/citrate ATPSs have been successfully used to purify Penicillin acylase [7], Plasmid DNA [8] and amylase [9] with recoveries higher than 80%. In our laboratory, PEG (MW3350)/sodium citrate pH 5.20 ATPSs have been used to recover the 60% of trypsin with 3-fold purification from bovine pancreas [10]. Systems formed by PEG600 and sodium tartrate have been found to be adequate to recover most of pancreatic trypsinogen and chymotrypsinogen (76% and 87%) practically free of cell debris, nucleic acids and lipids [11].

In this work, we evaluate the performance of PEG/sodium citrate ATPSs in purifying bromelain (BR) and papain (PAP), two well-known cysteine-proteases, with multiple applications in food,

* Corresponding author. Tel.: +54 0341 4804592; fax: +54 0341 4804598.
E-mail address: bnerli@fbioyf.unr.edu.ar (B.B. Nerli).

0141-8130/$ – see front matter © 2013 Elsevier B.V. All rights reserved.
http://dx.doi.org/10.1016/j.ijbiomac.2013.06.055

leather and pharmaceutical industries. BR is obtained from the stem of *Anana Comosus* while PAP source is the latex of *Carica papaya*. Traditional purification of BR and PAP involves a complex sequence of clarification, acetone/ammonium precipitation and successive chromatographic steps that are time-consuming and no eco-friendly. Both proteases exhibit structural and chemical similarities such as molecular weight (approximately 23,000), isoelectric point (close to 9.60) and amino acid sequences. Both BR (from fruit juice) and PAP have been successfully purified by applying PEG/potassium phosphate and PEG/ammonium sulfate ATPSs [12,13]. Nowadays, however, there exists a huge interest in developing more eco-friendly systems due to the high eutrophication potential of ammonium and phosphate ions [6] and the consequent negative impact in the environment.

The aim of this study was to analyze those variables that affect the partitioning equilibrium of PAP and BR in ATPSs formed by polyethyleneglycol (PEG) and sodium citrate (NaCit) pH 5.20 in order to assess the potential of such systems for a possible use in downstream process. At this pH value both proteases are stable and citrate solutions exhibit buffer capability, making this variable keep constant at different working conditions.

Thermodynamic characterization of the partitioning process, spectroscopy measurements and computational calculations of protein surface properties were also carried out in order to explain their differential partitioning behavior irrespective of their structural similarities. This information could contribute to a better understanding of the mechanisms involved in protein partition and therefore, to a rational design of extraction protocols with ATPSs.

2. Materials and methods

2.1. Chemicals

Polyethyleneglycols of average molecular weights (MW): 600, 1000, 2000, 4600 and 8000 (PEG600, PEG1000, PEG2000, PEG4600, PEG8000), alpha-*N*-benzoyl-DL-arginine-*p*-nitroanilide (BAPNA) and alpha-N-carbobenzyloxy-L-lysine p-nitro-phenyl ester (LNPE) and used without further purification. All other reagents were of analytical quality.

2.2. Proteins

Papain (PAP) from latex of *Carica papaya*; bromelain (BR) from the stem of *Anana Comosus* were also purchased from Sigma Chem. Co. Stock solutions of both proteases were prepared by weighting appropriate quantities of commercial enzymes until a final concentration of approximately 4000 μM. PAP was dissolved in 100 mM sodium phosphate buffer pH 6.00 while BR was dissolved in 100 mM sodium acetate buffer pH 5.00, EDTA 100 mM and KCl 0.3 M in order to prevent the enzyme degradation. Both solutions were kept at −18 °C. Measurements of enzyme activities (see below) were carried out before using to check the eventual loss of protein structural integrity with the storage.

2.3. Enzyme activity assays

Bromelain activity was determined by using the substrate LNPE [14]. This substrate was used in the assay at a final concentration of 0.23 mM in 30 mM buffer NaAc pH 4.6 100 mM KCl. Cysteine was added to the cuvette at a final concentration of 0.96 mM for full activation of the enzyme. The activity was monitored by direct spectrophotometric measurement of the enzyme-catalysed hydrolysis of LNPE at 340 nm for 5 min.

Papain was determined by measuring its amidase activity against the chromogenic reagent BAPNA [15]. This substrate was used in the assay at a final concentration of 0.95 mM in 500 mM buffer NaPi pH 7.00, 100 mM cysteine (to activate enzyme). The reaction was followed by measuring the absorbance of the released reaction product, p-nitroanilide, at 400 nm for 10 min.

Both enzyme assays were performed at constant temperature of 25 °C. The activities were calculated from the initial linear portion of the absorbance vs. time curve.

2.4. Effect of PEG presence on structure of BR and PAP

2.4.1. Fluorescence and circular dichroism measurements

Effect of PEGs (5 and 10%, w/w) of different molecular weight on intrinsic protein fluorescence was evaluated. Both enzymes, PAP and BR at a final concentration in cuvette of 17.33 μM, were excited at 280 and 290 nm and the emission was recorded from 300 to 500 nm. PEG solutions were prepared in buffer sodium phosphate 50 mM pH 6.00. Fluorescence measurements were performed on an Aminco Bowman S2 spectrofluorometer using a thermostatized cuvette of 1 cm of optical pathway. Emission spectra were corrected using the software supplied by the manufacturer.

Circular dichroism spectra (CD) were performed in a Jasco J-810 spectropolarimeter. Far-UV CD spectrum (195–245 nm) was recorded by using a thermostatized cuvette of 1 mm of pathlength, the scan rate was of 100 nm min^{-1} and the bandwidth was of 10 nm. Repetitive scanning of eight cycles was used. Near-UV CD spectra were measured with a 10 mm path length cuvette in the region of 250–320 nm to study the changes in the tertiary structure. Results are expressed as mean residue ellipticity [θ] calculated as:

$$[\theta] = \frac{\theta_{obs}}{10\,nCl} \quad (1)$$

where θ_{obs} is the CD in milli-degree, n is the number of amino acid residues, l is the path-length of the cell in cm, and C is the protein molar concentration. Final protein concentration in cuvette was 23.0 μM for BR and 11.5 μM for PAP in far-UV and 21.6 μM for both enzymes in near-UV region. PEG concentration was 5% (w/w) in all cases.

2.4.2. Changes in enzyme activity

The enzyme activity of both proteases was used to monitor the structural integrity (functionality) of protein in presence of PEGs of different sizes. Solutions of both BR and PAP at final concentration 43 μM and 200 μM, respectively, were incubated for 0, 60, 120 and 180 min with PEG solutions 30% (w/w) at 20 °C. The activity was then determined according to the protocol described in Section 2.3. All the measurements were developed by triplicate. The activity mean value was determined in each case. The results were presented as the residual activity (expressed in percentage) relative to the activity of the enzyme in absence of polymer at initial time.

2.5. Calculation of surface properties of BR and PAP

The accessible superficial area for the amino acid of type i, ASA_i, and the total accessible superficial area of a given protein, ASA_{prot}, was calculated by using the free software SURFACE RACER [16] and the PDB files with the three-dimensional of protein structure were downloaded from the National Center for Biotechnology Information web site (http://www.ncbi.nlm.nih.gov/sites/entrez).

The protein surface hydrophobicity, $\phi_{surface}$, was calculated with the following equation:

$$\phi_{surface} = \sum_{i \in A} r_i \phi_i \quad (2)$$

where ϕ_i is the hydrophobicity of the amino acid of type i and A is the collection of the 20 possible amino acids. It was proposed

by Berggren et al. [17] and assumed that each amino acid in the protein surface contributes, proportionally to its abundance, with properties associated to the protein surface. The hydrophobicity of each amino acid (ϕ_i) was computed according to the scale of Cowan–Whittaker [18] in which values assigned to the most hydrophilic and the most hydrophobic amino acid are −1 and +1 respectively. The fraction of protein superficial area, r_i occupied by the amino acid i is defined by:

$$r_i = \frac{\sum_{i \in A} \mathrm{ASA}_i}{\mathrm{ASA}_{\mathrm{prot}}} \quad (3)$$

2.6. Partitioning measurements

2.6.1. Determination of partition coefficients of PAP (Kp_{PAP}) and BR (Kp_{BR})

Aqueous two phase systems of total mass 2 g were prepared by weighing and mixing adequate quantities of stock solutions of the phase components: PEGs of different molecular weight 30% (w/w) and sodium citrate 25% (w/w) pH 5.20. Two different compositions were assayed for each PEG molecular weight according to binodal diagram determined previously in our laboratory [19]. They were identified by the numbers 1 and 2 according to their increasing tie line length. Table 1 shows the total and phase compositions of the selected systems.

Partitioning behavior of BR and PAP was analyzed by dissolving a given amount (100 μL) of stock solution of protein (4350 μM) in the prepared two-phase systems (2 g). This aliquot is small enough to prevent changes in binodal compositions. After mixing by inversion for 15 min and leaving it to settle for at least 60 min, the system was centrifuged 5 min at low speed (2000 rpm) for two-phase separation. Appropriate amounts were removed from each phase and assayed for enzyme activity. Partition coefficients of BR and PAP (Kp_{BR} and Kp_{PAP}) were calculated from their enzyme activity (Act) at the top and bottom phases according to the following equation:

$$\mathrm{Kp} = \frac{\mathrm{Act}_{\mathrm{top}}}{\mathrm{Act}_{\mathrm{bottom}}} \quad (4)$$

Temperature was maintained constant and controlled to within ±0.1 °C by immersing the glass tubes in a thermostatic bath. All the measurements were developed by triplicate. The mean Kp value and its estimated mean error was informed in each case.

2.6.2. Determination of thermodynamic functions associated to the protein partitioning

BR and PAP partition coefficients (Kp_{BR} and Kp_{PAP}) were determined at different temperatures (T) in the range 15–35 °C. By applying an integrated version of van't Hoff equation:

$$\ln\ \mathrm{Kp} = -\frac{\Delta H^\circ}{R}\frac{1}{T} + \mathrm{constant} \quad (5)$$

the enthalpy change (ΔH°) associated to the protein partitioning was calculated from the slope of a ln Kp vs. $1/T$ plot. The free energy change (ΔG°) was determined from:

$$\Delta G^\circ = -\mathrm{RT}\ \ln \mathrm{Kp} \quad (6)$$

and the entropy change (ΔS°) from:

$$\Delta S^\circ = \frac{\Delta H^\circ - \Delta G^\circ}{T} \quad (7)$$

All the thermodynamic parameters were calculated with mean Kp values from triplicate measurements.

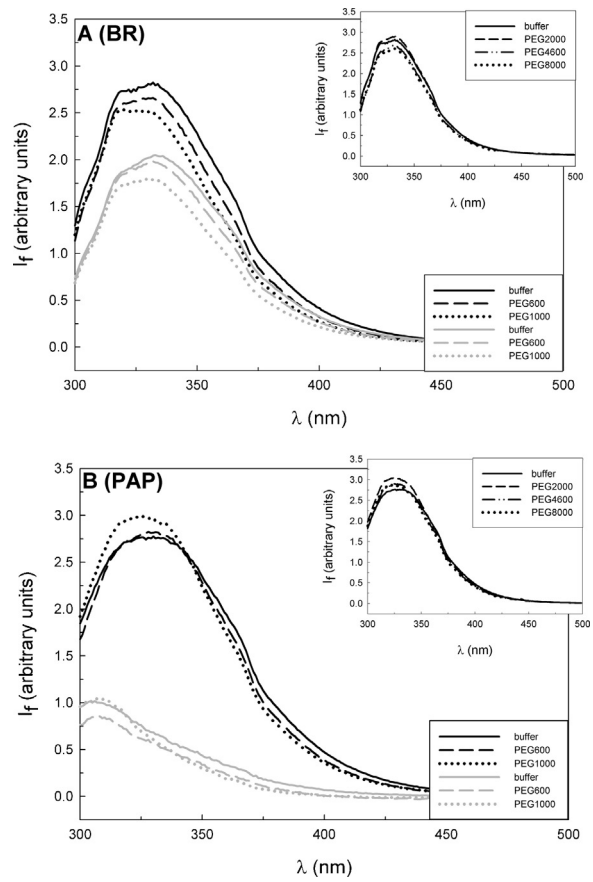

Fig. 1. Effect of PEGs (10%, w/w) of different molecular weight on emission spectrum of BR (A) and PAP (B). Final protein concentration 17.33 μM, λ_{exc} 280 nm (in black), λ_{exc} 290 nm (in gray). Temperature 20 °C.

3. Results and discussion

3.1. Effect of PEG on protein structure

Fluorescence spectroscopy was used to monitor changes on the tertiary structure induced by the interaction with PEG. These interactions can, *a priori*, produce changes in the position or orientation of the tryptophan residues, altering their exposure to solvent and therefore, leading to alterations either on the quantum yield or the position of emission maximum. Tryptophan residues dominate the fluorescence because both their absorbance at the wavelength of excitation and their quantum yield of emission are considerably higher than the respective values of the rest of amino acids able to have fluorescence emission (tyrosine and phenylalanine) [20]. Fig. 1A shows the emission spectra of BR in buffer phosphate pH 6.00 and in the presence of PEGs (10%, w/w) of different average MW. A comparison of the emission observed after excitation at 280 and 290 nm shows that the shapes of the fluorescence spectra are virtually identical, thus suggesting that the measured emission originates almost completely from the Trp residues. In the absence of PEG, the BR spectrum exhibits a main peak at 332 nm and a shoulder at lower wavelength (approx. 320 nm), which may be explained by the presence of tryptophan residues with different exposure in the molecule. Some of them, buried in the hydrophobic core of protein which emit at lower wavelength- and the others, located near the surface of the molecule. Table 2 shows the accessible superficial area of different types of amino acid in BR calculated according to Section 2.5. Stem bromelain contains five tryptophan residues. Those at positions 8 and 27 exhibit low ASA while the other three are clearly more exposed. According to Fig. 1A, most

Table 1
Total, bottom and top composition of ATPSs formed by PEGs of different molecular weights and NaCit pH 5.20.

PEG molecular weight	TLn	Total composition (%, w/w)			Bottom composition (%, w/w)			Top composition (%, w/w)		
		PEG	NaCit	H_2O	PEG	NaCit	H_2O	PEG	NaCit	H_2O
600	1	18.55	15.26	66.19	2.89	23.56	73.55	37.03	5.47	57.5
	2	21.00	16.20	62.80	0.77	27.89	71.34	42.65	3.69	53.66
1000	1	15.00	13.20	71.80	11.23	14.92	73.85	20.09	10.88	69.03
	2	15.92	13.97	70.11	5.10	19.01	75.89	28.87	7.47	63.66
2000	1	13.25	11.20	75.55	2.13	16.28	81.59	26.26	5.25	68.49
	2	13.75	14.40	71.85	0.13	21.59	78.28	36.78	2.24	60.98
4600	1	11.39	9.02	79.59	2.01	12.80	85.19	18.05	6.33	75.62
	2	11.70	9.65	78.65	0.88	14.18	84.94	23.92	4.53	71.55
8000	1	10.82	8.83	80.35	3.08	11.81	85.11	18.87	5.73	75.4
	2	11.69	9.52	78.79	1.44	13.52	85.04	24.19	4.63	71.18

Table 2
The accessible surface area (ASA) of tryptophan (Trp), Lysine (Lys), histidine (His) and arginine (Arg) residues calculated with SURFACE RACER software for BR and PAP.

Aminoacid	ASA (Å^2)			
	BR		PAP	
Trp	353.75	(5)	194.60	(5)
^{8}Trp	15.56	^{7}Trp	23.63	
^{27}Trp	1.55	^{26}Trp	12.11	
^{67}Trp	139.73	^{69}Trp	82.96	
^{176}Trp	111.99	^{177}Trp	59.05	
^{180}Trp	84.92	^{181}Trp	16.85	
Lys	2057.25	(15)	742.21	(10)
His	46.58	(1)	26.75	(2)
Arg	595.99	(6)	1288.85	(12)

of the assayed PEGs (PEG600, PEG1000. PEG4600 and PEG8000) quenches the fluorescence intensity. Particularly, the shoulder at 320 nm, in PEG1000 presence, is practically not affected but fluorescence intensity at the main peak (332 nm) is decreased. This suggests that only the surface-exposed tryptophans are quenched, leading to a greater proportion of the remaining signal coming from the most buried tryptophans (^{8}Trp and ^{27}Trp) that are located in the interior of the native protein. Probably, the hydrogen bonding and hydrophobic interactions between PEGs and BR lead to changes in the microenvironment around external Trp, thus inducing the quenching effect. The presence of PEG2000 does not affect the fluorescence spectrum (inset). Probably, for this PEG, a compensation of the opposite effects hydrogen bonding and increasing hydrophobic character of tryptophan environment- would be taking place.

The PAP spectrum (Fig. 1B) in the absence of PEG shows one peak at 330 nm. This behavior agrees with a low exposure (see ASAs in Table 2) of their five tryptophan residues. In this case the spectrum in presence of PEG600 is superimposed to that corresponding to buffer medium. The presence of the rest of PEGs enhances fluorescence signal and induces a little shift to lower wavelengths compatible with an increase in hydrophobic character of fluorophore environment.

Circular dichroism spectra of proteins are known to be sensitive to protein secondary structure [21]. Fig. 2A and B shows the effect of PEGs at a concentration of 5% (w/w) on far-UV dichroism spectrum of BR and PAP. The spectral characteristics displayed by both proteins are typical of $\alpha + \beta$ proteins, i.e. two bands, one positioned at 222 nm and the other at 208 nm. These features can be appreciated in all the spectra, thus evidencing that both proteins retain their ordered secondary structure even in the presence of PEGs.

The near-UV CD spectrum (250–320 nm) of proteins arises from the contributions of the environments of each aromatic amino acid side chain. In this context, tryptophan, tyrosine and phenylalanine have characteristic peaks close to 290, 275 and 255 nm respectively [22]. Fig. 3A and B shows the CD spectra of BR and PAP in this

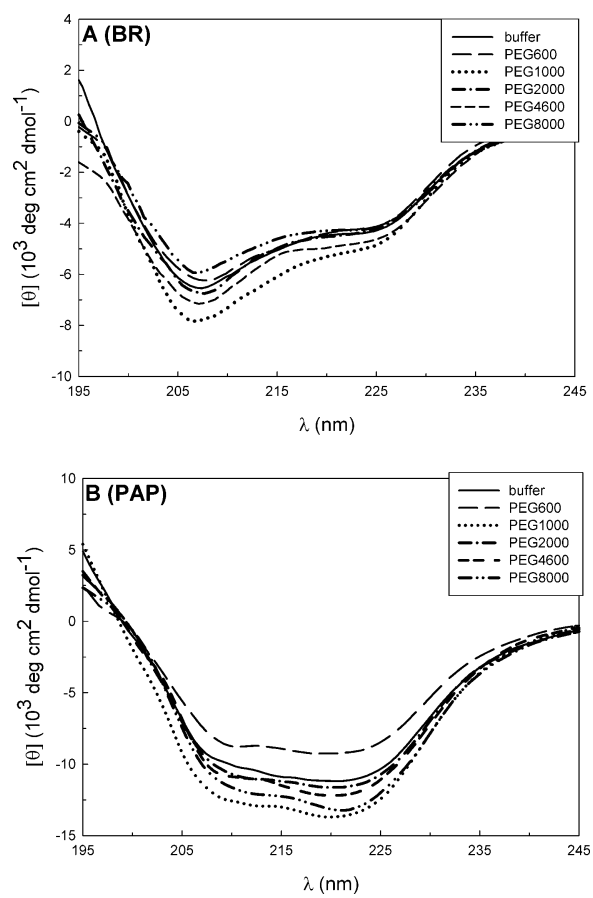

Fig. 2. Effect of PEGs (5%, w/w) of different molecular weight on far-UV DC spectrum of BR 23 μM (A) and PAP 11.5 μM (B). Buffer sodium phosphate 50 mM pH 6.00. Temperature 20 °C.

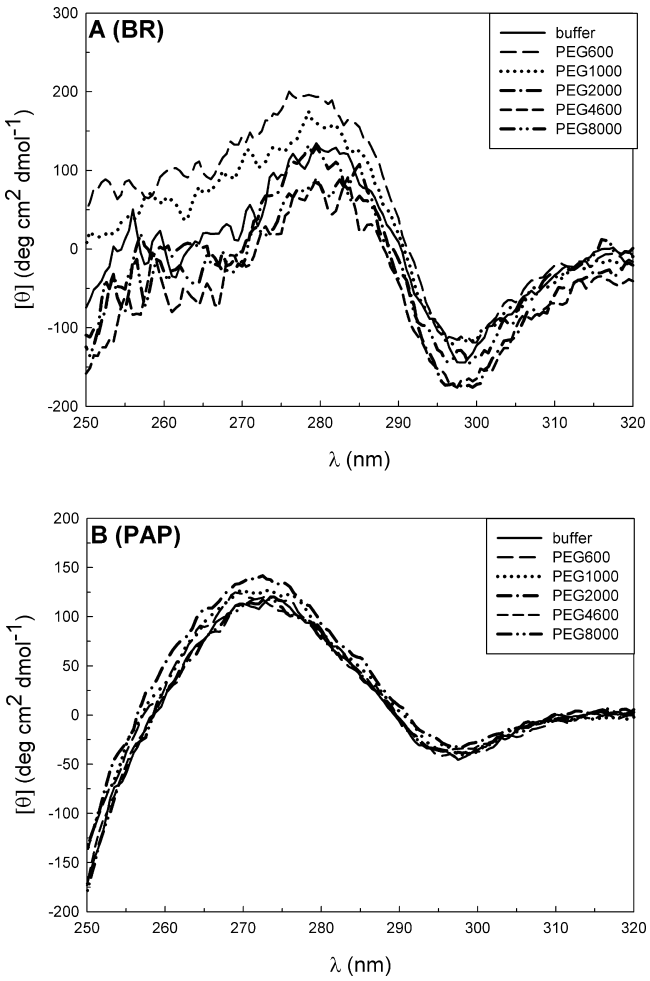

Fig. 3. Effect of PEGs (5%, w/w) of different molecular weight on near-UV DC spectrum of BR (A) and PAP (B). Final protein concentration 21.6 μM. Temperature 20 °C.

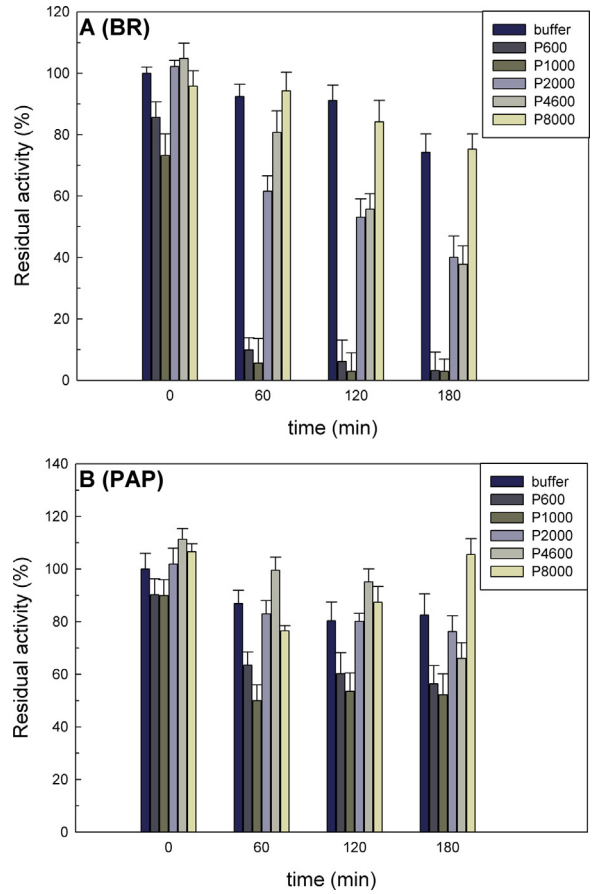

Fig. 4. Progress of enzymatic activity of BR 43 μM (A) and PAP 200 μM (B) with time in presence of PEGs (30%, w/w) of different molecular weight. Residual activity is calculated considering activity obtained in absence of polymer at initial time as 100%. Temperature 20 °C. The mean estimated errors of enzyme activities are indicated on each bar Temperature 20 °C.

region. Clearly, it can be appreciated that PEG600, and PEG1000 perturb the CD signal of BR, suggesting that these PEGs induce micro-arrangements at the aromatic amino acid residues accessible to solvent. No effect is observed for PAP in all the cases.

Fig. 4A and B shows the effect of PEGs on the enzyme activity of BR and PAP through time. After an incubation period of three hours, the activity of BR and PAP in buffer decreases up to 70 and 80% respectively. Presence of PEG led to different patterns. While BR showed a drastic decrease of activity in the presence of PEG600 and PEG1000, PAP retained at least a 50% of activity in all cases, irrespective of their molecular weight. The behavior observed for BR suggests the PEG–protein interaction would be affecting the active site through two possible mechanisms: PEG molecules bind to the protein at the active site, thus blocking the substrate binding; PEG molecules bind to protein in sites different from active site but induces conformation changes which affect the conformation of active site, and therefore, the enzyme activity. Activity of BR and PAP in presence of PEG8000 showed results either comparable or enhanced respect to those observed in buffer medium. This agrees with an unspecific exclusion of this polymer from protein surface and a consequent structure-stabilizing effect, predicted by Timasheff theory.

3.2. Partitioning measurements

Fig. 5 depicts the partitioning behavior observed for both phytoproteases in different systems. The increase in PEG molecular weight produces a decrease in Kp_{PAP} and Kp_{BR}, BR being more sensitive than PAP to this variable. This trend seems to be a general rule in protein partition process and could be attributed to a reduction of the space available for proteins when the polymer chain length increases. Particularly, BR exhibits drastic changes in the

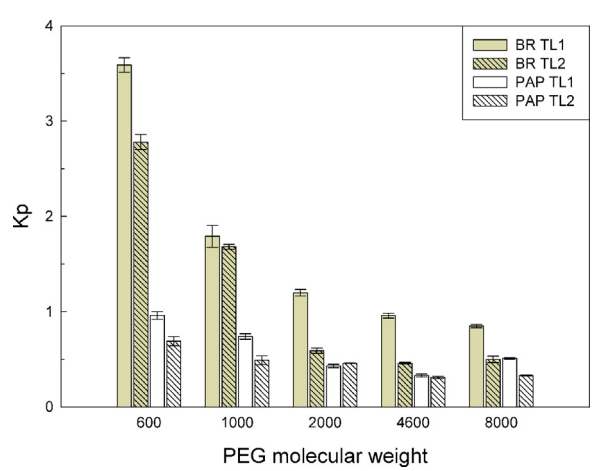

Fig. 5. Partitioning pattern of BR and PAP in aqueous two-phase systems formed by sodium citrate pH 5.20 and PEGs of different molecular weight. Composition of two tie lines (1 and 2) are showed in Table 1. Each Kp is the average of three independent measurements. The mean estimated error for the partition coefficients is indicated on each bar. Temperature 20 °C.

Kp values (close to five times for TL2) when the PEG MW varies from 600–1000 (Kp ⋙ 1) to 2000 (Kp < 1). Most of the BR is recovered in the top phase of PEG600/PEG1000 ATPSs with yields close to 76 and 63% respectively. *A priori*, these systems seem to be appropriate for first downstream steps since other significant components present in stem bromelain (the main source), such as polysaccharides and particulate matters usually partition to the salt-enriched phase [23]. However, the drastic loss of enzymatic activity observed in presence of these PEGs limits their use in recovering strategies. Reversibility of inactivation process should be evaluated in order to overcome this disadvantageous feature. Changes observed in Kp_{PAP} when PEG MW is varying are not so significant. The partitioning equilibrium of PAP is displaced to the bottom phase in most of the assayed systems with Kp values close to 0.50. Partition coefficients of both BR and PAP increases by decreasing the concentration of phase components, i.e. in systems with low tie line lengths. This effect is not relevant enough to make PAP being unevenly transferred to the top phase since Kp_{PAP} is lower than 1 even in PEG600 and PEG1000 ATPSs. Besides, systems with composition of too short tie lines are not desirable due to the risk of becoming one phase systems after loading complex mixtures such as homogenates, cell cultures and crude supernatants [24].

From a rough inspection of Fig. 5, a general trend can be stated, i.e. the partitioning equilibrium of BR is more displaced to the top phase than that of PAP in all the assayed systems. This effect is more pronounced in systems containing PEG600 and PEG1000 in which an uneven distribution is observed. The following empirical expression can be used to understand this behavior [25]:

$$\log \text{Kp} = \log K_{\text{hydroph}} + \log K_{\text{elec}} + \log K_{\text{size}} + \log K_{\text{affinity}} + \log K_{\text{SBAcompos}} \quad (8)$$

This equation considers all the factors that affect protein partitioning. $K_{SBAcompos}$ denotes the contribution of system properties, i.e. type, MW and concentration of phase components. $K_{hydroph}$, K_{size} and K_{elec} are related to the properties of partitioned molecule such as surface hydrophobicity, size (it includes MW and conformation) and net electrical charge respectively. Finally, $K_{affinity}$ is related to the presence of a specific interaction between the target molecule and phase components. When comparing the values of Kp_{BR} and Kp_{PAP} in similar SBAs, $K_{SBAcompos}$ remains constant. Therefore, the observed differences between Kps are expected to be related to other factors. It is well-known that stem BR possesses extensive sequence homology with PAP [26]. Both enzymes exhibit similar molecular weights (23,000) and isoelectric points (9.60), therefore, the terms $\log K_{elec}$ and $\log K_{size}$ are not expected to be responsible for the higher Kp_{BR} values.

The surface hydrophobicity ($\phi_{surface}$), calculated according to Eq. (2), evidenced a hydrophobic character slightly higher for BR (−0.0318) than for PAP (−0.0363), suggesting a more favorable interaction of BR with non polar rests such as ethylene groups in PEG. This argument seems reasonable to explain the little differences in Kp values of BR and PAP in systems formed by PEG of high MW (more hydrophobic ones) but seems inconsistent to explain the major differences between Kp_{BR} and Kp_{PAP}, observed for PEGs with lower hydrophobic character, i.e. PEG600 and PEG1000. We speculate that in these cases, an additional specific interaction BR-PEG would be taking place thus making the term $\log K_{affinity}$ become significant. Thermodynamic parameters associated with protein transfer to the top phase were calculated in order to identify the driven forces involved in the partitioning process (Fig. 6). Ln Kp vs. $1/T$ plots showed linearity for BR and PAP in the temperature range assayed (data not shown), thus indicating that the enthalpy change, calculated from its slope, keeps constant within this interval. Clearly, the transfer of PAP to the polymer phase is associated

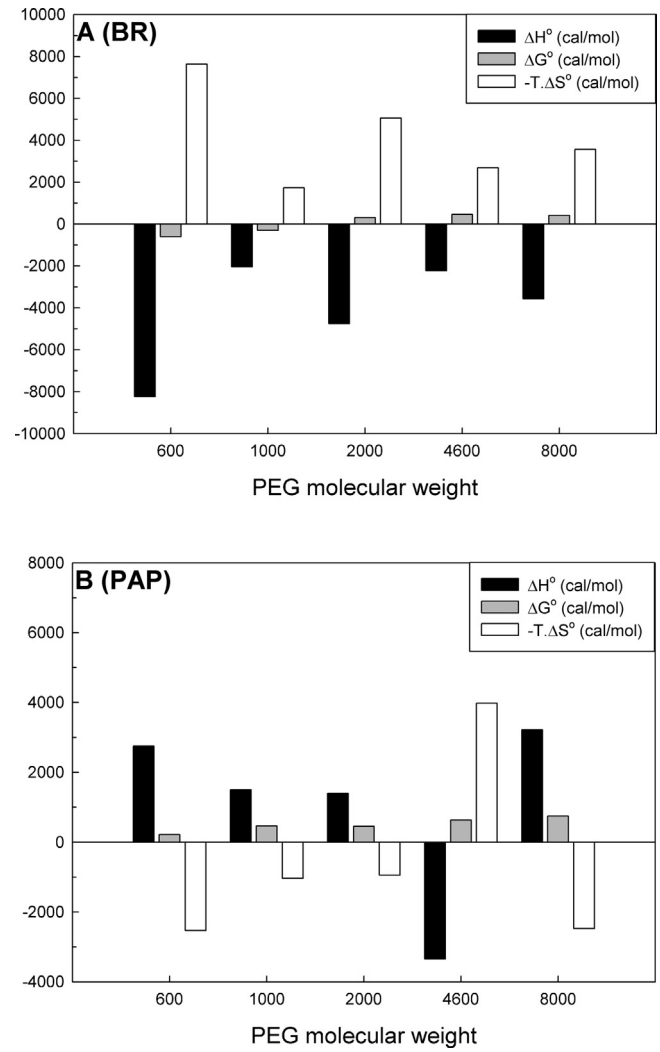

Fig. 6. Thermodynamic parameters associated to the transfer of BR and PAP to the top phase of aqueous two-phase systems formed by sodium citrate pH 5.20 and PEGs of different molecular weight. Composition corresponding to tie line number 2.

to low positive changes in both enthalpy and entropy values (Fig. 6 B). This trend, also obtained for the partition of chymotrypsinogen and trypsinogen in PEG/sodium tartrate systems [27], appears to be the thermodynamic manifestation of the structuring/destructuring effect of water molecules in the partitioning mechanism. At bottom phase (salt-enriched), the hydrophobic regions on PAP surface are in contact with a solvation shell formed by water molecules more structured (lesser mobile) than water molecules of bulk. When protein is transferred to the top phase (polymer-enriched), van der Waals forces take place as a result of fluctuations in the charges of proteins and dipoles or multipoles in the polymer. As a consequence, rupture of hydrogen bonds ($\Delta H^{\circ} > 0$) from the structured water in their neighbors [28] and an increase in the system disorder ($\Delta S^{\circ} > 0$) are produced. This "hydrophobic effect", observed for PAP is represented in Fig. 7.

BR exhibit an opposite thermodynamic pattern with significant negative changes in both enthalpy and entropy values, characteristic features of enthalpically driven processes (Fig. 6A).

This suggests the presence of an additional mechanism different from the hydrophobic effect, involved in protein transfer to the polymer phase. Berggren et al. [25] found that the presence of exposed aromatic residues in monomeric proteins had a strong effect on its partition coefficient in EO30PO70/dextran systems,

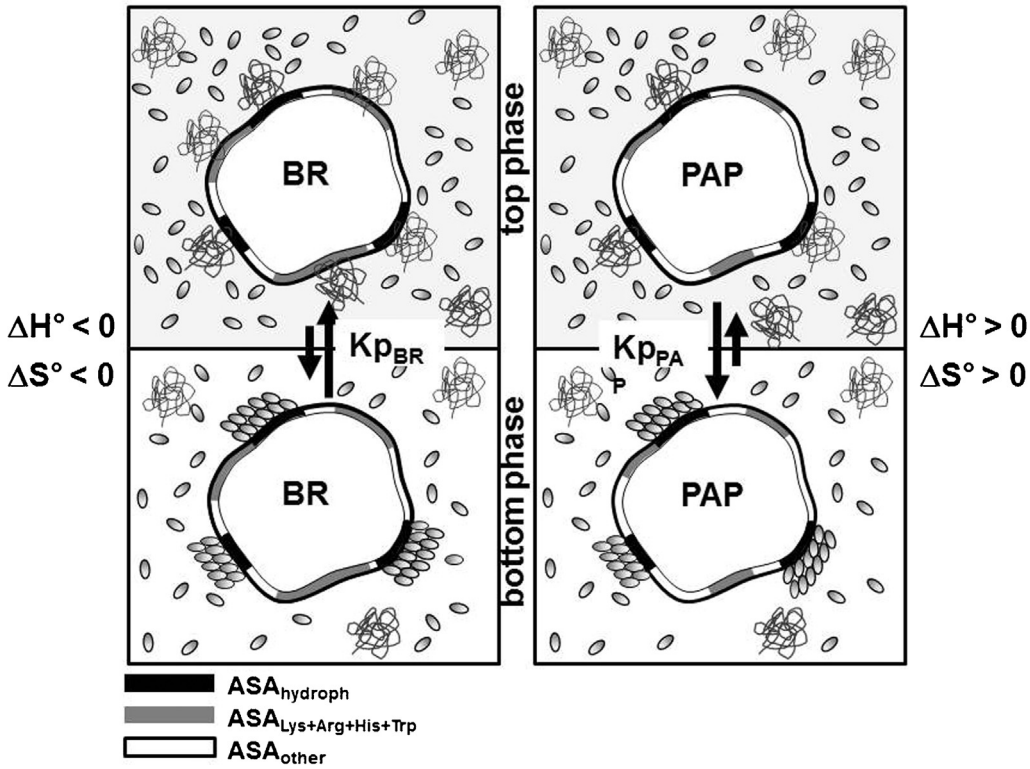

Fig. 7. Schematic representation of mechanism involved in partition of BR and PAP in aqueous two-phase systems formed by sodium citrate pH 5.20 and PEGs of low molecular weight.

giving preference to the upper (more hydrophobic) phase. Particularly, the presence of certain amino acid rests, such as tryptophans, exposed in the protein surface, have been reported [29] to enhance drastically the protein partition to the polymer phase. A selective charge transfer interaction between PEG and tryptophan, in which the pirrole nitrogen of the indole ring would be a hydrogen donor, has been postulated. In addition, crystallographic studies [30] stated that the main PEG–protein surface interactions could include multiple coordination contacts of oxo groups in PEG to positively charged lysine, arginine and histidine residues (take into account that p*Ka* of these amino acids are higher than 5.20, the working pH). According to Table 2, the total number of basic amino acids is similar for both enzymes (24 for PAP and 22 for BR). However, the degree of exposure of them is quite different, the higher exposed area being observed for BR. An analog behavior exhibit the Trp rests which practically duplicate the exposed area in BR, as it was previously discussed in this section. As a consequence of these structural features, BR presents enhanced chances to interact with PEG by charge transfer mechanism in addition to the "hydrophobic effect". This fact would be responsible of negative enthalpy and entropy changes associated to BR partitioning and would be crucial to determine its uneven partition in PEG600-PEG1000/citrate ATPSs. Fig. 7 also shows the postulated mechanism for BR partitioning. In this case, the higher exposed area of Trp and basic amino acids (Lys, His and Arg) would facilitate the formation of PEG-BR complex, thus displacing the partitioning equilibrium to the top phase.

4. Conclusions

ATPSs formed by sodium citrate and PEGs of higher molecular weights, particularly PEG8000, showed to be the most appropriate ones to be included in purification protocols since they allow to recover most of the target proteins at the salt-phase without affecting their enzymatic activity. Systems formed by PEG600 and PEG1000 lead to high BR yields, however, the inhibitory effect of these PEGs on enzymatic activity represent a critical concern.

Our results allow us to propose a mechanism for BR and PAP partitioning in the PEG/citrate pH 5.20 ATPSs comprised of general effects observed for other protein-ATPS such as the exclusion due to the polymer size and the "hydrophobic effect". In systems formed by PEG of low MW (PEG600 and PEG1000) a relevant role can be assigned to the content of highly exposed tryptophan and positively charged residues (Lys, Arg and His), amino acid rests responsible for a charge transfer PEG-protein interaction and therefore, for the uneven distribution of BR in these systems.

Acknowledgements

This work was supported by a grant from CONICET PIP0196. We thank Maria Robson for the language correction of the manuscript.

References

[1] P.Å. Albertsson, Partition of Cell Particles and Macromolecules, 2nd ed., John Wiley and Sons, New York, 1971.
[2] M. Rito Palomares, Journal of Chromatography B 807 (2004) 3–11.
[3] M. Rito-Palomares, A. Lyddiatt, Chemical Engineering Journal 87 (2002) 313–319.
[4] B.Y. Zaslavsky, Aqueous Two-Phase Partitioning. Physical Chemistry and Bioanalytical Applications, Marcel Dekker Inc., New York, 1994.
[5] H. Walter, D.E. Brooks, D. Fisher, Partitioning in Aqueous Two-Phases Systems, Academic Press Inc., Orlando, 1985.
[6] M. Perumalsamy, T. Murugesan, Fluid Phase Equilibria 244 (2006) 52–61.
[7] J.C. Marcos, L.P. Fonseca, M.T. Ramalho, J.M.S. Cabral, Enzyme and Microbial Technology 31 (2002) 1006–1014.
[8] F. Rahimpour, F. Feyzi, S. Maghsoudi, R. Hatti-Kaul, Biotechnology and Bioengineering 95 (2006) 627–637.
[9] W. Zhi, J. Song, F. Ouyang, J. Bi, Journal of Biotechnology 118 (2005) 157–165.
[10] G. Tubio, G. Picó, B.B. Nerli, Journal of Chromatography B 877 (2009) 115–120.
[11] L. Pellegrini Malpiedi, G. Picó, B. Nerli, Separation and Purification Technology 78 (2011) 91–96.

[12] B. Ravindra Babu, N.K. Rastogi, K.S.M.S. Raghavarao, Chemical Engineering and Processing 47 (2008) 83–89.
[13] S. Nitsawang, R. Hatti-Kaul, P. Kanasawuda, Enzyme and Microbial Technology 39 (2006) 1103–1107.
[14] R.L. Heinrikson, F.J. Kézdy, Methods in Enzymology 45 (1976) 740–751.
[15] M. Azarkan, R. Dibiani, C. Baulard, D. Baeyens-Volant, International Journal of Biological Macromolecules 38 (2006) 216–224.
[16] O.V. Tsodikov, M.T. Record Jr., Y.V. Sergeev, Journal of Computational Chemistry 23 (2002) 600–609.
[17] K. Berggren, M. Egmond, F. Tjerneld, Biochimica et Biophysica Acta 1481 (2000) 317–327.
[18] R. Cowan, R.G. Whittaker, Peptide Research 3 (1990) 75–80.
[19] Tubío G., L. Pellegrini, G. Picó, B.J. Nerli, Chemical & Engineering Data 51 (2006) 209–212.
[20] J. Lakowicz, Principles of Fluorescence Spectroscopy, Plenum Press, NY, 1983.
[21] N. Sreerama, R. Woody, Protein Science 12 (2003) 384–388.
[22] S. Kelly, N. Price, Current Protein and Peptide Science 1 (2000) 349–384.
[23] D.P. Harris, A.T. Andrews, G. Wright, D.L. Pyle, J.A. Asenjo, Bioseparation 7 (1997) 31–37.
[24] P. Selvakumar, T.C. Ling, S. Walker, S. Lyddiatt, Journal of Chromatography B 878 (2010) 1784–1790.
[25] K. Berggren, A. Wolf, J. Asenjo, B. Andrews, F. Tjerneld, Biochimica et Biophysica Acta 1596 (2002) 253–268.
[26] K.L. Lee, K.L. Albeee, R.J. Bernaschoni, T. Edmunds, Biochemical Journal 327 (1997) 199–202.
[27] L. Pellegrini Malpiedi, G. Picó, W. Loh, B. Nerli, Journal of Chromatography B 878 (2010) 1831–1836.
[28] M. Harris, Poly(ethylene glycol) Chemistry. Biotechnical and Biomedical Applications, Plenum Press, New York, 1992.
[29] J. Huddleston, A. Veides, K. Köhler, J. Flanagan, S-O. Enfors, A. Lyddiatt, Trends in Biotechnology 9 (1991) 381–388.
[30] J. Hasek, Zeitschrift für Kristallographie Supplements 23 (2006) 613–618.